Inkjet Printing of Carbon Nanospheres

M. Orrill*, D. Abele**, N. Banek**, M. Wagner**, and S. LeBlanc*

*Department of Mechanical and Aerospace Engineering
**Department of Chemistry
The George Washington University
800 22nd St. NW Ste 3000, Washington, DC, USA, sleblanc@gwu.edu

ABSTRACT

Proposed applications of drop-on-demand inkjet printing extend beyond printing of text and graphics to include rapid manufacturing of thin and flexible electrical devices. Typical inks for printed electronics are made with silver or gold nanoparticles, so they are expensive and require post-processing to recover high conductance. The post-processing step restricts substrate material selection and process throughput. Cheaper metal nanoparticles such as aluminum and copper share these limitations, and they are highly susceptible to oxidation, limiting electrical conductance. Here we synthesize an inkjet-printable ink with hollow carbon nanospheres consisting of concentric graphene spheres. Ink properties relevant for inkjet printing (viscosity, zeta potential, and particle size distribution) are characterized, and initial printing trials are demonstrated.

Keywords: inkjet, carbon, nanoparticles, flexible electronics

1 INTRODUCTION

Over the last few decades inkjet printing has become a major topic in scientific research, particularly drop-on-demand inkjet printing. Applications for the technology have extended beyond printing of text and graphics to rapid manufacturing of thin devices [1]. A major area of interest is flexible electronics that enable novel designs for devices including smartphones, televisions, photovoltaics, sensors, and biological implants. Printing processes are attractive for electronic devices because printing is cheaper than traditional electronic fabrication processes, which require lithography, chemical etching and deposition. Another advantage is material versatility and diversity of inks and substrates. Since printing technologies have been in regular use since the 1970s, there is a well-established base of manufacturing expertise. Printing can produce multiple complex devices at high resolution over large areas on different substrate types in a solution-based, non-contact, mask-less, and additive process.

Inkjet printing of electronic materials is hindered by the synthesis of printable inks, compatibility of inks with flexible substrates, and the electrical performance of printed materials. The most commonly printed electronic material is silver, but there are several drawbacks including its high cost and low as-printed conductance. Silver inks require a post-processing step (e.g., thermal annealing) to recover some fraction of bulk silver's conductivity. This post-processing step restricts substrate material selection and process throughput. These limitations are shared by other traditional electronic materials such as copper, gold, and aluminum. Oxidation of nanoparticles is another significant problem and can severely reduce or prevent electrical conductance, especially for copper and aluminum, which necessitates specialized processing and handling.

Functional electronic inks are multiphase solid-liquid (sol) colloidal suspensions. An ideal printable electronic ink should be inexpensive and made with environmentally benign solvents (water, alcohols, etc.). The solid particles should be stable, without sedimentation, aggregation, or chemical reactions. The printed material should form highly electrically conductive traces with excellent adherence after solvent evaporation with minimal post-processing.

A new class of materials, hollow carbon nanospheres (HCNS) are promising for use in electronic ink formulations. They are the byproduct of a biofuel production process from charred cellulose, an agricultural waste product generated by fast growing plants such as switchgrass. Because switchgrass requires no tending and thrives on marginal, arid land, its economic impact is small. Thus, HCNSs are inexpensive, and their production could reduce the cost of biofuels and serve as a carbon sink. HCNS are chemically stable and have high electrical conductivity. Their diameter can be controlled through synthesis conditions, and they can easily be dispersed into alcohols, water, and other solvents to form stable colloids. Chemical modification to improve adhesion or add functionality is also possible with conventional synthesis methods. These characteristics make HCNS an ideal material for electronic inks [2].

This work aims to create a printable and stable ink with HCNS. The particles are treated to maximize colloidal stability and particle concentration. Relevant ink properties—viscosity, zeta potential, and dispersed particle size distribution—are characterized. Printing parameters are determined, and initial printing trials are carried out.

2 INKJET PRINTING

Inkjet printing as a non-contact, maskless, and additive manufacturing process is suitable for the fabrication of thin and flexible electronics and sensors. There are two mechanisms of drop-on-demand printing, thermal bubble

jet and piezoelectric. Piezoelectric printheads are better suited for functional inks because they do not depend on the boiling point of inks, and some ink formulations may be sensitive to large thermal fluctuations.

The critical properties for inks in piezoelectrically driven printheads are the fluid density, viscosity, and surface tension. Ejection of droplets results from the superposition of consecutive acoustic waves imparted to the fluid by a piezoelectric transducer. The acoustic waves create pressure pulses large enough to overcome viscous dissipation and the energy required to form a new surface. The acoustic wave speed in the ink depends on its density. Viscosity dampens excess acoustic waves and fluid motion to reset the system between each pulse. The viscosity and surface tension balance in ejected jets of fluid to ideally form a single droplet [3].

3 METHODS

3.1 Particle Synthesis

The HCNS material was prepared by initially mixing 10 g of microcrystalline cellulose (Avicel PH-105 NF, FMC BioPolymer) with 2 g of $NiCl_2$ in a hardened steel cup (80 mL, Fritsch GmbH) with six hardened steel balls (1 cm diameter, Fritsch GmbH) at 300 rpm for 30 min using a planetary mill (Pulverisette 6, Fritsch GmbH). The resulting powder was pressed at 10,000 psi into a 20 mm diameter pellet, and a 1/4" hole was drilled in its center with a drill press. The pellet was then heated under N_2 gas from room temperature at a 10 °C min^{-1} ramp rate to 375 °C and held for a total heating time of 30 min. After cooling, the charred pellet was skewered on a 1/4" diameter stainless steel rod which was then placed vertically into a stainless steel 4-way cross, fed through the top flange equipped with an Ultra-TorrTM vacuum fitting (Swagelok), and secured to a stepper motor (STM-23, Applied Motion Products). The chamber was evacuated to 10^{-3} torr and maintained at 0.5 torr with flowing He. The pellet was then irradiated by a 2 mm diameter 10.4 µm laser beam (Firestar t60, Synrad Inc.) while rotating at a linear velocity of 1.63 mm s^{-1} (1.2 rev min^{-1}) for one full rotation. The surface of the pellet exposed to the laser was removed by gentle abrasion, and the resulting powder was purified by reflux in HNO_3 using a MARS 5 Digestion Microwave System (CEM Corp.). The pellet was heated from room temperature to 190 °C over 10 min ramp and held at that temperature for 40 minutes. After cooling under ambient conditions, the mixture was diluted with deionized water, and the HCNS powder was collected by vacuum filtration (P8 cellulose fiber, Fisher Scientific) and the process repeated until a neutral pH was obtained. Finally, the HCNS sample was washed with 1 M NaOH and neutralized again by repeatedly rinsing with deionized water.

The HCNS sample was further oxidized by a modified Hummers method [4]. HCNSs (180 mg) were added to concentrated H_2SO_4 (5 mL) contained in a 100 mL round bottom flask chilled to 0 ˚C with an ice bath. $KMnO_4$ (300 mg) was slowly added while monitoring temperature with an alcohol thermometer; the rate of addition was adjusted to maintain the solution temperature below 20 °C. The reaction mixture was then heated to 40 °C and stirred for 30 minutes. Deionized water (10 mL) was added and stirred for an additional 15 minutes after the temperature had been raised to 95 °C. Additional deionized water (35 mL) was added, followed by 1 mL of H_2O_2 dropwise. The oxidized HCNS were then filtered and washed with 0.1 M HCl solution, followed by repeated rinsing with deionized water until a neutral pH was obtained. Subsequently, the HCNS sample was washed with 1 M NaOH and neutralized again by repeatedly rinsing with deionized water. Finally, the oxidized HCNS were dried under vacuum.

The HCNS tend to agglomerate which is undesirable for inkjet printing since large particles can clog printhead nozzles. Figures 1 and 2 show transmission electron microscope and scanning electron microscope images of agglomerated particles. The concentric graphene rings can be seen in the close up in Figure 1 (right).

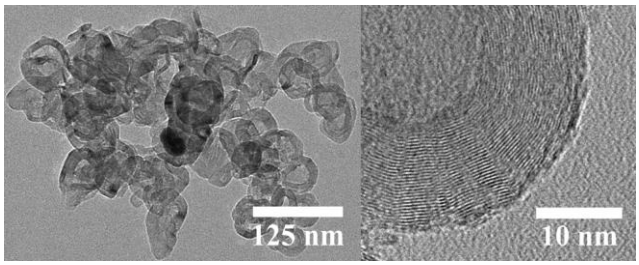

Figure 1: Transmission electron microscope image of HCNS agglomerate (left) and concentric graphene spheres of a HCNS shell (right).

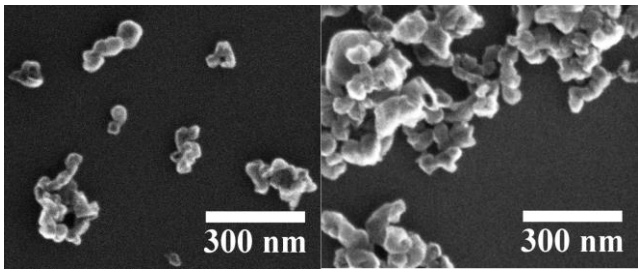

Figure 2: Scanning electron micrographs showing small (left) and large (right) agglomerates of HCNS.

3.2 Ink Preparation

Dried HCNS powder was ground using a mortar and pestle then added to neat ethylene glycol under vigorous stirring in a ratio of 5 mg/mL. The mixture was stirred for 10 minutes at 1200 rpm and then dispersed using a horn ultrasonicator (Fisher Scientific FB-505) while immersed in an ice bath for 20 minutes with 10 second pulses and rests at an amplitude of 20%. The resulting mixture was

centrifuged for 10 minutes at 7500 rpm. The supernatant was separated, dried, and weighed in order to calculate the final ink concentration of the ink, 2.8 mg/mL. The viscosity, particle size distribution and zeta potential were then measured.

3.3 Ink Characterization

Shear rates experienced in inkjet printheads range from $0 – 10^6$ s^{-1} [3]. To fully characterize the viscosity, it should be measured over the entire applicable range to identify any non-Newtonian behavior [5]. Viscosity was measured as a function of shear rate in a rotational rheometer (TA Instruments, Discovery HR-2) with a 1° cone/flat plate geometry. The hygroscopic nature of ethylene glycol necessitated the use of a solvent trap to limit the solvent's exposure to air. The use of the solvent trap reduced the testable shear rate range in the rotational rheometer to ~ 2,000 s^{-1}. Another rheometer based on microfluidics (Rheosence, mVROC) allowed for measurements up to 23,000 s^{-1}. The HCNS ink showed Newtonian behavior for the range of shear rate tested, and the results are shown in Table 1. The printable range of viscosity varies between printheads. For the printer used in this study (FUJIFILM, Dimatix DMP 2381) the printable range of viscosity is 2 – 30 mPa.s although optimal values are 10-12 mPa.s.

Property	Measured value	Unit
Average viscosity	15.16 ± 0.19	mPa.s
Average particle size	119.3 ± 1.1	nm
Zeta potential	-56.5 ± 2.7	mV

Table 1: Measured properties of HCNS ink.

Particle size distribution and zeta potential were measured by dynamic light scattering (Malvern, Zetasizer Nano ZS). The average particle size and zeta potential are listed in Table 1. The particle size distribution is shown in Figure 3 below.

Based on the transmission and scanning electron micrographs in Figures 1 and 2 and the particle size distribution in Figure 3, the solution is composed of agglomerates consisting of 2 – 4 HCNS. Since the full width, half maximum of the size distribution is 118.5 nm, most agglomerates are 80 to 198 nm in size. The printhead manufacturer recommends that particles should be less than 1/100 of the diameter of the printhead nozzles to avoid clogging. The approximate diameter of the printhead nozzles used in this work is 21.5 µm corresponding to a maximum recommended particle size of 215 nm.

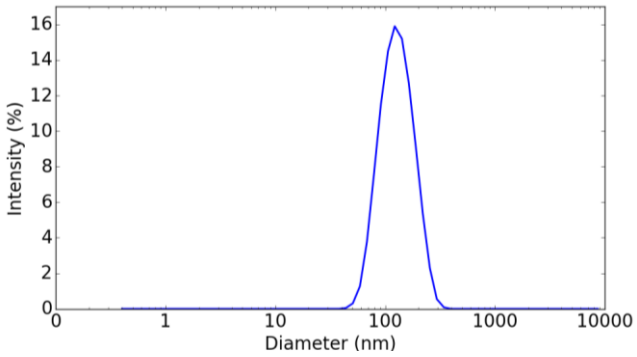

Figure 3: Particle size distribution.

The zeta potential is a measure of the electrical potential between the surface of a dispersed particle and the surrounding liquid. The electrical potential of one particle interacts with that of other particles producing a repulsive force if both particles have the same charge. This repulsive force stabilizes particles against agglomeration. The Derjaguin–Landau–Verwey–Overbeek (DLVO) theory for colloids indicates the barrier height of the potentials determines the stability with respect to the kinetic energy, k_BT, of the particles (where k_B and T are the Boltzmann constant and absolute temperature, respectively). If the repulsive potential is much greater than k_BT, then the suspension will be stable. In general, particles with a zeta potential greater than 30 mV or less than -30 mV are considered electrostatically stable [6].

The measured zeta potential of the HCNS ink, -56.5 ± 2.7 mV, indicates that the suspension is stable. In fact, particles have remained dispersed in ethylene glycol for seven months. Additionally, the zeta potential can be increased, and thus the stability improved, by changing the pH of the solution.

3.4 Printing trials

The prepared ink was printed using a Dimatix materials benchtop inkjet printer. First, a driving waveform was designed by adjusting the shape, amplitude, and duration of the applied voltage for each ink nozzle. Ejected droplets were observed stroboscopically while the waveform was adjusted until stable, single droplets of desirable volume and velocity were achieved. Figure 4 shows an image from the stroboscopic drop watcher camera. While droplet ejection appeared stable, ink can wet the nozzle plate near the nozzle orifices, causing subsequent droplets to change trajectory. This results in poor print quality as can be seen in Figure 5. The printhead is periodically cleaned during the printing process to improve print quality. Other printing parameters include the printhead height from the substrate, droplet spacing, and substrate temperature. Lines of ink were printed onto glass slides in 1, 10, and 25 layers. The substrate was kept at room temperature for the 1 layer line and 60 °C for the others with 40 second delays between layers.

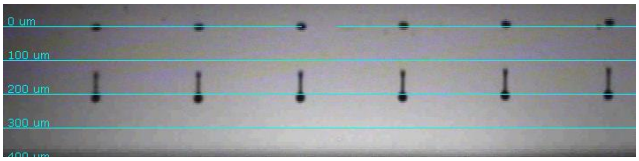

Figure 4: Snapshot from stroboscopic drop watcher camera showing ejected droplets of HCNS ink.

Examples of common printing defects are shown in bright and dark field optical microscope images of the printed lines in Figure 5. The concentration of HCNS in the ink is too low to form a continuous track of carbon material with fewer than 10 printed layers. Poor line continuity is caused by large droplet spacing or variability of the velocity and direction of ejected droplets. The coffee ring effect is caused by internal flows that carry solid particles to the periphery and center of ink deposits. Coffee ring mitigation methods include electrowetting, surfactant-induced Marangoni flows and eddies, and by trapping particles at the liquid-gas interface with enhanced hydrophobicity of oppositely charged surfactant-particle systems [3].

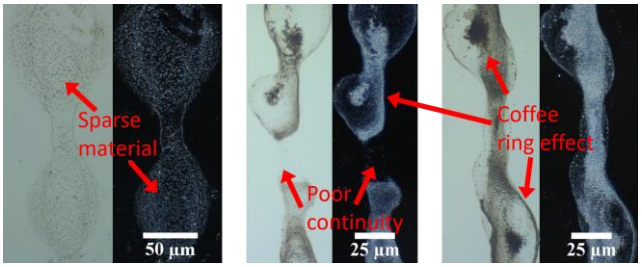

Figure 5: Bright and dark field images of printed HCNS ink in 1 layer (left), 10 layers (middle), and 25 layers (right)

In future work, the HCNS concentration in the ink should be increased to reduce the number of layers required to achieve a continuous track of solid material. By increasing the electrostatic repulsion between the carbon nanoparticles, their stability in the dispersion will be increased, and thus a higher concentration will be possible. This electrostatic repulsive force is characterized by the zeta potential and is dependent on the pH of the liquid phase.

4 CONCLUSIONS

An inkjet printable ink was created with a novel and environmentally friendly carbon nanomaterial. Important ink properties were characterized, and initial printing trials were carried out.

Ongoing work focuses on increasing the stability of HCNS in solution to achieve a higher concentration so that fewer ink layers are required to produce a continuous line of material. The zeta potential will be measured as a function of pH to identify the point at which zeta potential, and therefore particle stability, is maximized. The higher concentration ink will be characterized, including surface tension characterization. All printing parameters will be optimized, and test structures will be printed for electrical characterization. The innate versatility of carbon and the environmental benefit from the production of HCNS make this ink a promising alternative to traditional nanomaterial-based functional inkjet inks

REFERENCES

[1] T. H. J. Van Osch, J. Perelaer, A. W. M. De Laat, U. S. Schubert, Adv. Mater. 20, p. 343-345, 2008.

[2] M. J. Wagner, J. Cox, T. McKinnon, and K. Gneshin, U.S. Patent 8262942, issued September 11, 2012.

[3] M. Orrill, S. LeBlanc, J. Appl. Poly. Sci., 134, p. 44256, 2016.

[4] Chen, J., et al., Carbon, 64, p. 225-229, 2013.

[5] Duffy, J., Malvern Instruments, 2015. Available at: http://www.malvern.com/en/support/resource-center/Whitepapers/WP141027AnalyticInk.aspx

[6] T. K. Sen, C. Ray, Handbook of Surface and Colloid Chemistry, 4th Ed., CRC Press, p. 421, 2016.